Molecular Neurobiology (2020) 57:806–822
https://doi.org/10.1007/s12035-019-01745-z

Phosphodiesterase 7 Regulation in Cellular and Rodent Models of Parkinson's Disease

Jose A. Morales-Garcia[1,2,3] · Sandra Alonso-Gil[1,2] · Ángel Santos[2,4] · Ana Perez-Castillo[1,2]

Received: 4 June 2019 / Accepted: 19 August 2019 / Published online: 31 August 2019

Abstract

Parkinson's disease is characterized by a loss of dopaminergic neurons in the ventral midbrain. This disease is diagnosed when around 50% of these neurons have already died; consequently, therapeutic treatments start too late. Therefore, an urgent need exists to find new targets involved in the onset and progression of the disease. Phosphodiesterase 7 (PDE7) is a key enzyme involved in the degradation of intracellular levels of cyclic adenosine 3′, 5′-monophosphate in different cell types; however, little is known regarding its role in neurodegenerative diseases, and specifically in Parkinson's disease. We have previously shown that chemical as well as genetic inhibition of this enzyme results in neuroprotection and anti-inflammatory activity in different models of neurodegenerative disorders, including Parkinson's disease. Here, we have used in vitro and in vivo models of Parkinson's disease to study the regulation of PDE7 protein levels. Our results show that PDE7 is upregulated after an injury both in the human dopaminergic cell line SH-SY5Y and in primary rat mesencephalic cultures and after lipopolysaccharide or 6-hidroxydopamine injection in the *Substantia nigra pars compacta* of adult mice. PDE7 increase takes place mainly in degenerating dopaminergic neurons and in microglia cells. This enhanced expression appears to be direct since 6-hydroxydopamine and lipopolysaccharide increase the expression of a 962-bp fragment of its promoter. Taking together, these results reveal an essential function for PDE7 in the pathways leading to neurodegeneration and inflammatory-mediated brain damage and suggest novel roles for PDE7 in neurodegenerative diseases, specifically in PD, opening the door for new therapeutic interventions.

Keywords Astrocytes · Microglial cells · Neurodegeneration · Neuroinflammation · Parkinson · Phosphodiesterase7 · Regulation

Abbreviations

6-OHDA	6-Hydroxydopamine
AD	Alzheimer's disease
DAPI	4′,6-Diamidino-2-phenylindole
GFAP	Glial fibrillary acidic protein
LPS	Lipopolysaccharide
PD	Parkinson's disease
PDEs	Phosphodiesterases
PDE7	Phosphodiesterase 7
SNpc	*Substantia nigra pars compacta*
TH	Tyrosine hydroxylase

✉ Jose A. Morales-Garcia
jmorales@iib.uam.es

✉ Ana Perez-Castillo
aperez@iib.uam.es

[1] Instituto de Investigaciones Biomédicas (CSIC-UAM), Arturo Duperier, 4, 28029 Madrid, Spain

[2] Centro de Investigación Biomédica en Red sobre Enfermedades Neurodegenerativas (CIBERNED), Valderrebollo, 5, 28031 Madrid, Spain

[3] Departamento de Biología Celular, Facultad de Medicina, UCM, Avda. Complutense s/n, 28040 Madrid, Spain

[4] Departamento de Bioquímica y Biología Molecular, Facultad de Medicina, UCM, Avda. Complutense s/n, 28040 Madrid, Spain

Introduction

Neurodegenerative diseases are debilitating conditions strongly linked with age and characterized by a slow progressive loss of neurons in different areas of the brain, which finally leads to deficits in specific brain functions that causes movement disorders (ataxias) or mental functioning alterations (dementias). Amongst neurodegenerative diseases, dementias are responsible for the greatest burden of disease, with Alzheimer's disease representing most of the cases. Another neurodegenerative disease having a great impact on the quality of life of patients is Parkinson's disease (PD), which is

characterized by motor symptoms (tremor, rigidity or stiffness, bradykinesia or slowness of movement) and non-motor symptoms (visual hallucinations, dementia, etc.). Although the mechanism that drives chronic progression of neurodegenerative diseases remains elusive, several processes have been implicated in PD pathogenesis: aging, oxidative stress, mitochondrial dysfunction, protein misfolding and aggregation, glutamate excitotoxicity, and apoptosis [1].

Inflammation is a protective mechanism aimed to repair, remove the damaged tissues/cells, and repair the organisms after tissular damage, infective agents, parasites, or toxins [2]. Specifically, neuroinflammation is the protective mechanism in the central nervous system to restore the damaged neuronal cells mediated mainly by microglial cells [3]. In contrast to other neural cells, once the neurons are damaged or degenerated, they are unable to be repaired or regenerated in the central nervous system [4]. However, although at the beginning of a brain injury, glial cell activation can be protective [5], after a certain time, these cells (astrocytes as well as microglia) become over-activated and start releasing pro-inflammatory agents that further damage the neurons. Thus, currently, neuroinflammation is recognized as a critical component of neurodegenerative diseases, including PD [6–9]. In fact, activated glial cells have been detected in the *Substantia nigra pars compacta* (SNpc) of patients concurrently with an increased expression of pro-inflammatory mediators, leading to an inflammatory cycle that ultimately worsen the progression of the disease. In addition, different studies using preclinical models of PD indicate that inflammatory processes are instrumental in neuronal cell death [10–12]. Therefore, there is an urgent need to investigate more in deep those factors involved in the chronic activation of glial cells, worsening the progressive neurodegeneration that characterizes neurodegeneration.

Cyclic nucleotide phosphodiesterases (PDEs) are a large family of enzymes implicated in the metabolism of the 3′, 5′-cyclic nucleotides (cAMP and cGMP) [13]. The PDE superfamily consists of 11 subtypes (PDE1–PDE11) based largely on their sequence homology and is coded by 21 identified genes [14]. cAMP and cGMP are intracellular signaling molecules that mediate a huge variety of events in the central nervous system, including neurogenesis, the establishment of neuronal circuitry, apoptosis, plasticity, sleep, sensorimotor gating, mood stability, memory, and other cognitive functions [15]. Aging and age-related diseases, including Parkinson's disease, are associated with impairments in many, if not all, of these processes [16], suggesting that cyclic nucleotide signaling may be compromised in these patient populations. Moreover, elevation of intracellular cAMP level controls immunosuppressive and anti-inflammatory processes, and selective inhibitors of cAMP-specific PDEs have been widely analyzed as possible therapeutic agents for the treatment of human diseases [17–19]. Regarding PDE7, this enzyme is expressed in some regions of the brain, especially in Parkinsonism-related structures like striatum or *SN* [17, 20–23], which must be taken into account when designing new therapeutic strategies for the development of innovative treatments. In that sense, our group has previously described the neuroprotective and anti-inflammatory role of PDE7 inhibition in preclinical models of PD [24, 25]. Recently, we have described that PDE7 inhibition activates adult neurogenesis in vitro and in vivo [26]. Interestingly, PDE7 inhibition specifically promotes the formation of new dopaminergic neurons in an animal model of Parkinson's disease, which ameliorate the impaired neurogenesis that occurs as a consequence of the progress of the disease.

Nigrostriatal pathway controls the motor function, being cAMP one of the key intracellular mediators by binding to the striatal D_1 and D_2 dopamine receptors [27]. Therefore, PDE7 becomes a valuable therapeutic target to restore striatal dopamine signaling deficiencies, since its inhibition in the striatal postsynaptic terminals leads to an increase in cAMP levels, which in turn stimulates the levels of dopamine through the dopamine receptor–cAMP-mediated signaling [28]. Understanding how and why Parkinson's disease develops would provide novel strategies for a better treatment of this disease. In line with this, and taken into account the role of PDE7 inhibition in neurodegenerative diseases, in this work, we have aimed to an understanding of the mechanism through which this enzyme is regulated.

Methods

SH-SY5Y Cell Culture

SH-SY5Y human neuroblastoma-derived cells (Sigma) were cultured and propagated in RPMI (Sigma) supplemented with glutamine 2 mM (Sigma) and 10% of fetal bovine serum (FBS, Gibco), under standard conditions. Cells were seeded onto 100-mm culture plates (1.5×10^6 cells/plate) for Western blot analysis, onto 24-well plates (3×10^5 cells/well) for transient transfections and immunocytochemical analysis (1.5×10^5 cells/well), and onto 96-well plates (3×10^4 cells/well) for cell viability assay. On attaining semiconfluence, cells were treated with 6-OHDA (35 μM, Sigma) during 16, 24, 48, or 72 h.

Mesencephalic Mixed Neuron/Glia Cultures

Primary rat ventral mesencephalic neuron/glia cultures were prepared as previously described [24]. Briefly, ventral mesencephalic tissues were dissected from embryonic day 13/14 rats and dissociated with a mild mechanical trituration. Then, the supernatant was collected and centrifuged at 1200×*g*/5 min, and the pellet was resuspended and the cells were seeded onto 100-mm culture plates ($1{,}5 \times 10^6$ cells/plate) for Western blot

analysis or grown on glass coverslips in 24-well plates (5×10^5 cells/well) for immunocytochemical analysis. After 1 week in culture, cells were treated with LPS (10 μg/ml, Sigma) or 6-OHDA (35 μM, Sigma) for 16, 24, 48, or 72 h. Immunocytochemical analysis indicated that, at the time of treatment, the cultures were made up of 12% Iba1-immunoreactive (IR) microglia, 48% GFAP-IR astrocytes, and 40% Neu-N-IR neurons of which 2.8–3.8% were TH-IR neurons.

Primary Glial Cultures

Rat primary glial cultures were prepared from the cerebral cortex of 3-day-old rats as described previously [29]. Briefly, cerebral cortex was dissected, dissociated, and incubated with 0.25% trypsin/EDTA at 37 °C for 1 h. After centrifugation, the pellet was washed three times with HBSS (Gibco) and the cells were plated in poly-D-lysine (20 μg/ml) pretreated flasks (75 cm^2). After 7–10 days, the flasks were agitated in an orbital shaker for 4 h at 230 rpm at 37 °C and non-adherent microglial cells were isolated and plated onto 24-well plates (3×10^5 cells/well). Then, DMEM was added to the flasks, which were agitated in a horizontal shaker at 260 rpm at 37 °C. After overnight agitation, the supernatant (oligodendrocytes and some remaining microglial cells) was removed, and astrocytes (adherent cells) were collected and plated onto 24-well plates (3×10^5 cells/well). The purity of the cultures was > 95%, as determined by immunofluorescence analysis using an antiglial fibrillary acidic protein (GFAP; clone G-A-5; Sigma-Aldrich) antibody to identify astrocytes, an anti-Iba1 (Wako) antibody to identify microglial cells, and an anti-O4 (Millipore) antibody as a oligodendrocyte marker.

Cell Viability Assay

Cell viability was measured using the 3-(4,5-dimethylthiazol-2-yl)-2,5-diphenyltetrazolium bromide (MTT) assay kit (Roche Diagnostic, GmbH), based on the ability of viable cells to reduce yellow MTT to blue formazan. The extent of reduction of MTT was quantified by absorbance measurement at 595 nm according to the manufacturer's protocol. Each data point represents the mean ± SD of 6 replications in 3 different experiments.

Immunoblot Analysis

Total proteins were isolated from cell cultures using ice-cold RIPA buffer as described elsewhere [30]. A total amount of 30 μg of protein was subjected to 10% SDS-PAGE; then, the proteins were transferred into nitrocellulose membranes (Protran, Whatman). After blocking with 5% fat-free milk in Tris-buffered saline containing 0.1% Tween-20 for 1 h at RT, the membranes were incubated with different primary antibodies overnight at 4 °C according to standard procedures. A rabbit polyclonal anti-PDE7 (Proteintech) antibody was used. As a control, a mouse anti-α-tubulin (Sigma) antibody was used. The proteins were detected by chemiluminescence using an HRP substrate (GE Healthcare) after incubating the membrane with HRP-conjugated secondary antibody and washing with Tris buffered saline with Tween-20 (TBST). Secondary antibody was HRP-conjugated IgG goat anti-rabbit (Jackson Immunoresearch). Representative images of at least three independent experiments corresponding to three different samples are shown. The images of blotting were quantified using ImageJ software (Wayne Rasband, NIH, Bethesda, MD). Values in the text are the mean of at least three different experiments.

Immunocytochemistry

For immunofluorescence analysis, SH-SY5Y or primary mesencephalic cultures, grown on glass coverslips in 24-well cell culture plates, were fixed in phosphate-buffered saline (PBS) containing 4% paraformaldehyde (Sigma), blocked in PBS containing 0.1% Triton X-100 for 30 min at 37 °C, and incubated overnight at 4 °C with primary antibodies. The following antibodies were used: goat polyclonal anti-PDE7 (A-18, Santa Cruz Biotechnology), rabbit polyclonal anti-tyrosine hydroxylase (TH, Millipore), mouse monoclonal anti-Iba1 (Wako), and mouse monoclonal anti-GFAP (Sigma). Cells were then incubated for 45 min at 37 °C with appropriate Alexa Fluor 488- and 546-conjugated secondary antibodies (Jackson Immuno Research). Nuclei were stained with DAPI. Coverslips were mounted with Vectashield Mounting Medium (Vector Laboratories). Images were captured using a Zeiss LSM710 laser scanning spectral confocal microscope equipped with Plan-Apochromat 63X/1.4. Confocal microscope settings were adjusted to produce the optimum signal-to-noise ratio. To compare fluorescence signals from different preparations, settings were fixed for all samples within the same analysis. Representative images of at least three independent experiments are shown. A quantitative analysis of PDE7 expressing cells given a particular marker (TH, GFAP or Iba-1) was performed using the Image Pro software (Media Cybernetics, USA) and normalized to total nuclei (stained with DAPI). Areas to be counted were traced at high power (× 400), and at least four different counting fields were selected at random from six independent experiments of parallel cultures as previously described [31]. Results are expressed as a percentage of total dopaminergic (TH^+), microglial ($Iba1^+$), or astroglial ($GFAP^+$) cells co-expressing PDE7.

Promoter Cloning and Transient Transfections

A fragment of the human PDE7 promoter, from − 962/+ 109, was PCR-amplified from human genomic DNA using specific

primers and high-fidelity Eppendorf Triple Master PCR System (Eppendorf). The primers used were as follows: 5′-TGG GGA TTT TTC CAG AGT GGG-3′ (forward sequence) and 5′-CCC TGG GTG AGT AAC ACC AC-3′ (reverse sequence). The entire promoter fragment, P.PDE7/1071, was sequenced and subcloned in the promoterless luciferase reporter vector pxp1. For transient transfection experiments, semiconfluent SH-SY5Y cells and rat glial primary cultures were transfected with lipofectamine 2000 (Invitrogen) using the complete PDE7 promoter (2.5 μg DNA/well). Twenty-four hours after transfection, cells were harvested for determination of luciferase activity by using a reporter assay system (Promega, Madison, WI). β-Galactosidase was used to determine transfection efficiency. Each transient transfection experiment was repeated at least three times in triplicate. Some transfected cultures were stimulated with 6-OHDA (35 μM) or LPS (10 μg/ml) for 24 h; then, cultures were harvested for determination of luciferase activity as mentioned above.

Animals

All animal experiments were specifically approved by the "Ethics Committee for Animal Experimentation" of the Instituto de Investigaciones Biomedicas (CSIC-UAM) and carried out in accordance with the European Communities Council Directive (2010/63/EEC) and National regulations (normative 53/2013). Adult, male Wistar rats from our Animal facilities, weighing about 250 g, were housed in a cage (2–3 animals per cage for adults) with free access to food and water under a 12 h light/dark cycle. Special care was taken to minimize pain or discomfort of animals.

LPS and 6-OHDA Injection In vivo

The animals (four rats per experimental group) were anesthetized and placed in a stereotaxic apparatus (Kopf Instruments, CA). LPS (10 μg in 2.5 μl PBS) or 6-OHDA (9 μg in 2.5 μl PBS containing 0.05% ascorbic acid) were injected into the right side of the *SNpc* (coordinates from Bregma: posterior − 4.8 mm; lateral + 2.0 mm; ventral: + 8.2 mm, according to the atlas of Paxinos and Watson) [32]. Animals injected only with vehicle (basal group) were used as controls throughout all the in vivo experiments. After injection, animals were housed to recover and sacrificed 72 h after lesioning.

Fluorescent Immunohistochemical Analysis

Brains were processed as previously described [25]. Shortly, after animal perfusion with 4% paraformaldehyde, brains were removed, postfixed in the same solution at 4 °C overnight, cryoprotected in 30% sucrose, and frozen, and finally, 30-μm coronal sections were obtained using a cryostat. For immunohistochemistry, sections were incubated overnight at 4 °C with the appropriate primary antibody. Next day sections were washed thoroughly and subsequently incubated for 1 h at room temperature with appropriate Alexa Fluor 488- and 647-conjugated secondary antibodies (Jackson Immuno Research). For nuclear staining, sections were incubated with DAPI for 15 min at RT and then washed in PBS. Finally, brain slides were mounted in Vectashield H-1000 (Vector Laboratories). The following primary antibodies were used: goat polyclonal anti-PDE7 (A-18, Santa Cruz Biotechnology), rabbit polyclonal anti-tyrosine hydroxylase (TH, Millipore), rabbit polyclonal anti-dopamine transporter (DAT, Millipore), mouse monoclonal anti-DARPP32 (BD Bioscience), mouse monoclonal anti-GFAP (Sigma), and mouse monoclonal anti-Iba1 (Wako). Some sections containing the SNpc were used for caspase 3 active immunodetection in a triple immunofluorescence analysis. In that case, the primary antibodies used were goat polyclonal anti-PDE7 (A-18, Santa Cruz Biotechnology), mouse monoclonal anti-tyrosine hydroxylase (TH, Sigma), and rabbit polyclonal anti-caspase 3 active (R&D Systems) followed by the subsequent incubation with Alexa Fluor 488-, 546-, and 647-conjugated secondary antibodies (Jackson Immuno Research).

Cell Count Analysis and Densitometry

The number of dopaminergic neurons (TH-reactive cells), astroglia (GFAP-positive cells), or microglial cells (immunoreactive to Iba1) expressing PDE7 after injury, as well as the number of dopaminergic neurons co-expressing PDE7 and active caspase 3 in the *SNpc*, was estimated. To that end, a modified stereological approach was used as previously described [25]. Confocal images of serial coronal sections (30 μm) containing the entire SNpc (rostrocaudal extent) were acquired under an objective (× 63) to avoid oversampling errors. The number of positive cells was counted in a 1:6 series of sections, determining the boundaries of the *SNpc* with reference to internal anatomic landmarks [32]. Images were analyzed using computer-assisted image analysis software (Soft Imaging System Corporation, USA). Four rats per group were used. The total number of dopaminergic neurons, astroglial, and microglial cells in the *SNpc* expressing PDE7 or dopaminergic neurons expressing PDE7 together with active caspase 3 was determined by multiplying the average numbers of labeled cells/section by the total number of 30-μm-thick sections containing the SNpc. Data were expressed as a percentage, for a better understanding.

Optical densitometry was performed on coronal sections containing the striatum and immunostained with anit-TH, anti-DAT, or anti-DARPP32 antibodies using Image Pro software (Media Cybernetics, USA). The area of interest was delimited in the rostrocaudal axis in coronal slides 30 μm thick covering the whole striatal area. Images were acquired with a Zeiss LSM710 laser scanning spectral confocal

microscope equipped with a Plan-Apochromat 10×/0.45 DIC objective. In this system a motorized *x*, *y* axis enables to automatically capture multiple fields of view. The software offers tile Scan, in which small square grids of images are acquired to finally perform a whole striatal reconstruction. All lighting conditions and magnifications were held constant. After the whole striatal images (16 total) were stitched, color pictures were used in Fig. 5 and then converted to 8-bit greyscale images for quantification. For each animal, the average optical density was determined. The damage was calculated as the percent of the TH-, DAT-, or DARPP32-positive area in the lesioned striatum divided by the DAT-positive area of the untreated contralateral side.

Statistical Analysis

All numerical values are presented as mean ± standard deviation. Statistical significance was determined using 2-tailed *t*

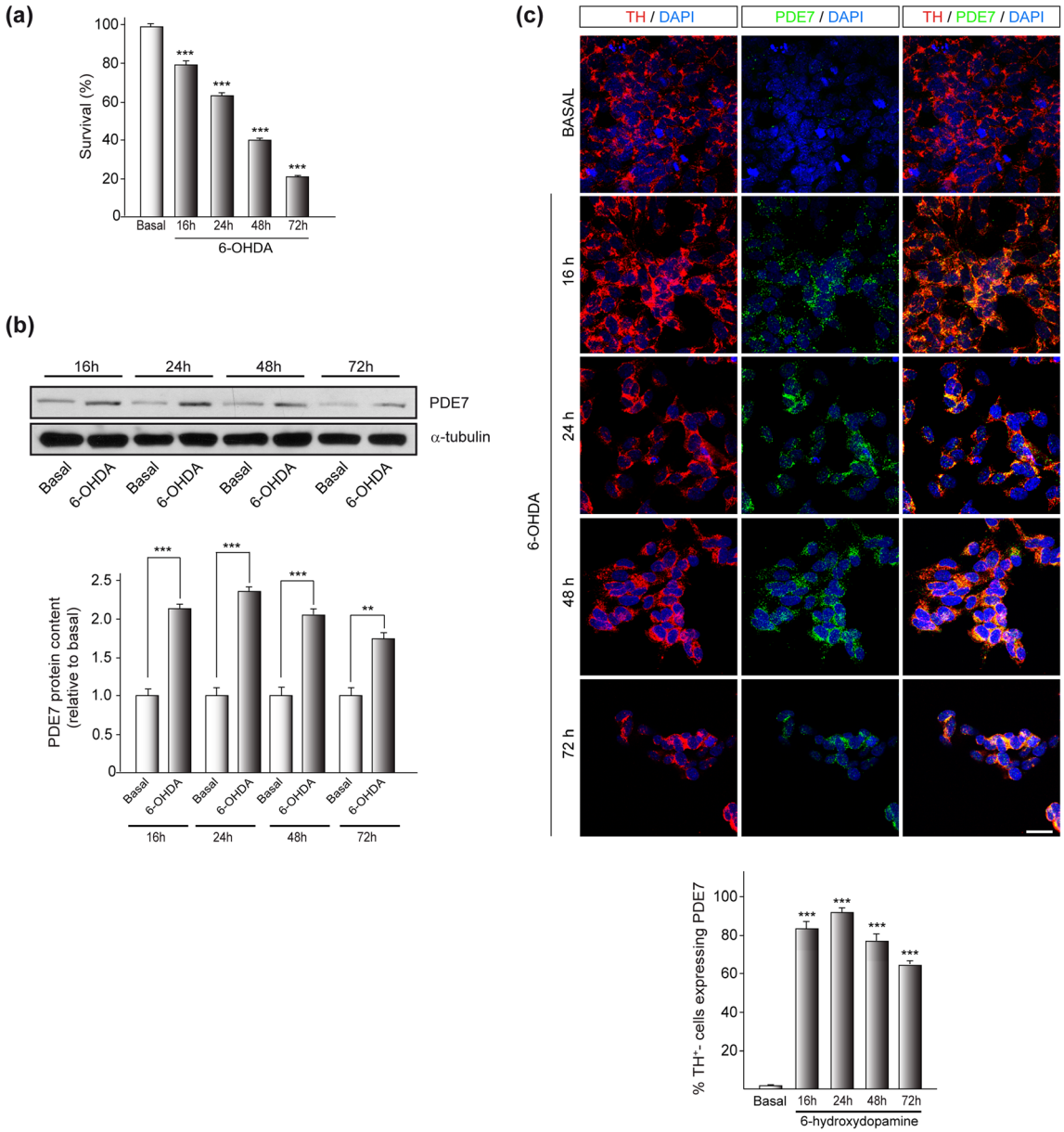

Fig. 1 PDE7 expression in the dopaminergic cell line SH-SY5Y after 6-OHDA-induced cell death. Cells were treated with 6-OHDA (35 μM) at indicated times. **a** Cell viability measurement after 6-OHDA treatment at indicated times. Values represent the mean ± SD of six replications in three different experiments. **b** Representative Western blot and quantification analysis showing expression levels of PDE7 in SH-SY5Y cells after damage. **c** Immunofluorescence analysis and quantification of PDE7 expression (green) and tyrosine hydroxylase (TH, red) in the dopaminergic cell line SH-SY5Y. Representative images of at least three independent experiments are shown. Scale bar, 20 μm. Nuclei were counterstained with DAPI (blue). Quantifications are expressed as a percentage of total dopaminergic (TH^+) cells co-expressing PDE7. ***$p \leq 0.001$; **$p \leq 0.01$ (basal-compared)

test analysis comparing the damaged group with control using SPSS version 12.0 (SPSS Inc., Chicago, IL, USA). p values < 0.05 were considered significant.

Results

PDE7 Expression Increases in Dopaminergic Cell Cultures After 6-Hydroxydopamine (6-OHDA)-Induced Death

6-OHDA causes a time-dependent decrease of cell viability in the human dopaminergic cell line SH-SY5Y; therefore, it is widely used for in vitro models of PD. We first analyzed PDE7 expression in dopaminergic cultures 16, 24, 48, and 72 h after 6-OHDA-induced death (Fig. 1). Numerous studies have described the importance of PDE7 in *striatum* and its relationship with Parkinson's disease [12, 33–35]. High concentrations of PDE7 mRNA are also found in those areas related to dopaminergic pathway, i.e., *Substantia nigra* and *striatum* [21, 23] and its expression is increased after dopamine D_1 receptor activation suggesting that PDE7 could be involved in the regulation of the signaling cascade initiated by this receptor [28]. To establish a time frame for the study of PDE7 expression, SH-SY5Y cell cultures were exposed to 6-OHDA during the times indicated above (Fig. 1a). As can be seen in this figure, SH-SY5Y cell survival diminished during the exposition to the neurotoxin. When PDE7 expression was analyzed in SH-SY5Y cultures by Western blot, high levels of PDE7 were found in the treated groups in comparison with low levels found in the basal state (Fig. 1b). Quantification analysis showed a significant increase in PDE7 protein levels starting at 16 h after damage. We next performed immunocytochemistry in these cultures after damage using a specific antibody against PDE7. Results summarized in Fig. 1c also showed an increased expression of PDE7 in dopaminergic neurons (TH-expressing cells) as a consequence of the treatment with 6-OHDA at all time points.

PDE7 Expression Increases in Embryonic Ventral Mesencephalic Cultures After Damage

Embryonic ventral mesencephalic cultures provide a useful tool for understanding the dopaminergic neuron properties and the pathways involved in the pathogenesis of Parkinson. These mixed cultures contain not only dopaminergic precursors but also glial cells, and can be subjected to various stress agents that mimic PD pathology and to neuroprotective compounds in order to stop or slow down neuronal degeneration. So next, some of these mixed cultures were treated with LPS to induce glial activation and therefore promote the initiation of neuroinflammatory processes. Other cultures were exposed to the neurotoxin 6-OHDA in order to damage specifically dopaminergic neurons. We have previously shown a low expression of PDE7 in basal conditions in these cultures [24]. To analyze the role of PDE7 in neurodegeneration and neuroinflammation, we first determined by Western blot the levels of PDE7 in embryonic ventral mesencephalic cultures 16, 24, 48, and 72 h after exposure to LPS or 6-OHDA. As can be observed in Fig. 2a, quantification of blots reveals a significant increase in PDE7 after damage suggesting that these mixed cultures, containing glial cells and dopaminergic neurons, were able to respond to injury increasing PDE7 levels in culture. Next, we performed double immunocytochemistry studies in embryonic ventral midbrain cultures in order to analyze which kind of cells, either dopaminergic neurons (Fig. 2b) or glial cells (Fig. 3), were expressing PDE7 in response to damage. Immunostaining with a specific dopaminergic marker (tyrosine hydroxylase, TH) together with an anti-PDE7 antibody revealed that after LPS- or 6-OHDA-damage, dopaminergic neurons in mesencephalic cultures were clearly expressing PDE7 (Fig. 2b). Similar results were obtained when midbrain cultures after exposure to LPS- or 6-OHDA were double immunostained with the microglial marker Iba-1 or GFAP to detect astrocytes. Figure 3 summarizes these results showing the expression of PDE7 in microglial cells and astrocytes after exposure to injury.

Fig. 2 PDE7 expression on embryonic mesencephalic-derived cultures after damage. Embryonic ventral mesencephalic cells were isolated, cultured, and treated with lipopolysaccharide (LPS, 10 μg/ml) or 6-hydroxydopamine (6-OHDA, 35 μM) at indicated times. **a** Representative Western blot and quantification analysis showing expression levels of PDE7 in mesencephalic cultures after damage. **b** Immunofluorescence analysis and quantification of PDE7 expression (green) in dopaminergic precursor cells (tyrosine hydroxylase positive cells, TH, red) on primary mesencephalic cultures after LPS- or 6-OHDA exposure at indicated times. Nuclei were counterstained with DAPI (blue). Scale bar, 20 μm. Representative images of at least three independent experiments are shown. Quantification results are expressed as a percentage of total dopaminergic (TH^+) cells co-expressing PDE7. $^{***}p \leq 0.001$ (basal-compared)

Brain-Derived Glial Culture Response to Injury Increasing PDE7 Expression After Damage

PDE7 expression is increased in glial cells (astrocytes as well as microglia) derived from mixed embryonic mesencephalic cultures after different insults, promoting neuroinflammation that eventually leads to dopaminergic cell death. Thus, we next wonder whether pure primary glial cultures derived from adult brain rats subjected to a cellular damage will also increase the expression of PDE7. To that purpose, we isolated and cultured separately brain-derived microglial cells and astrocytes. Each type of culture was treated for 16, 24, 48, and 72 h with LPS and PDE7 detection was performed by

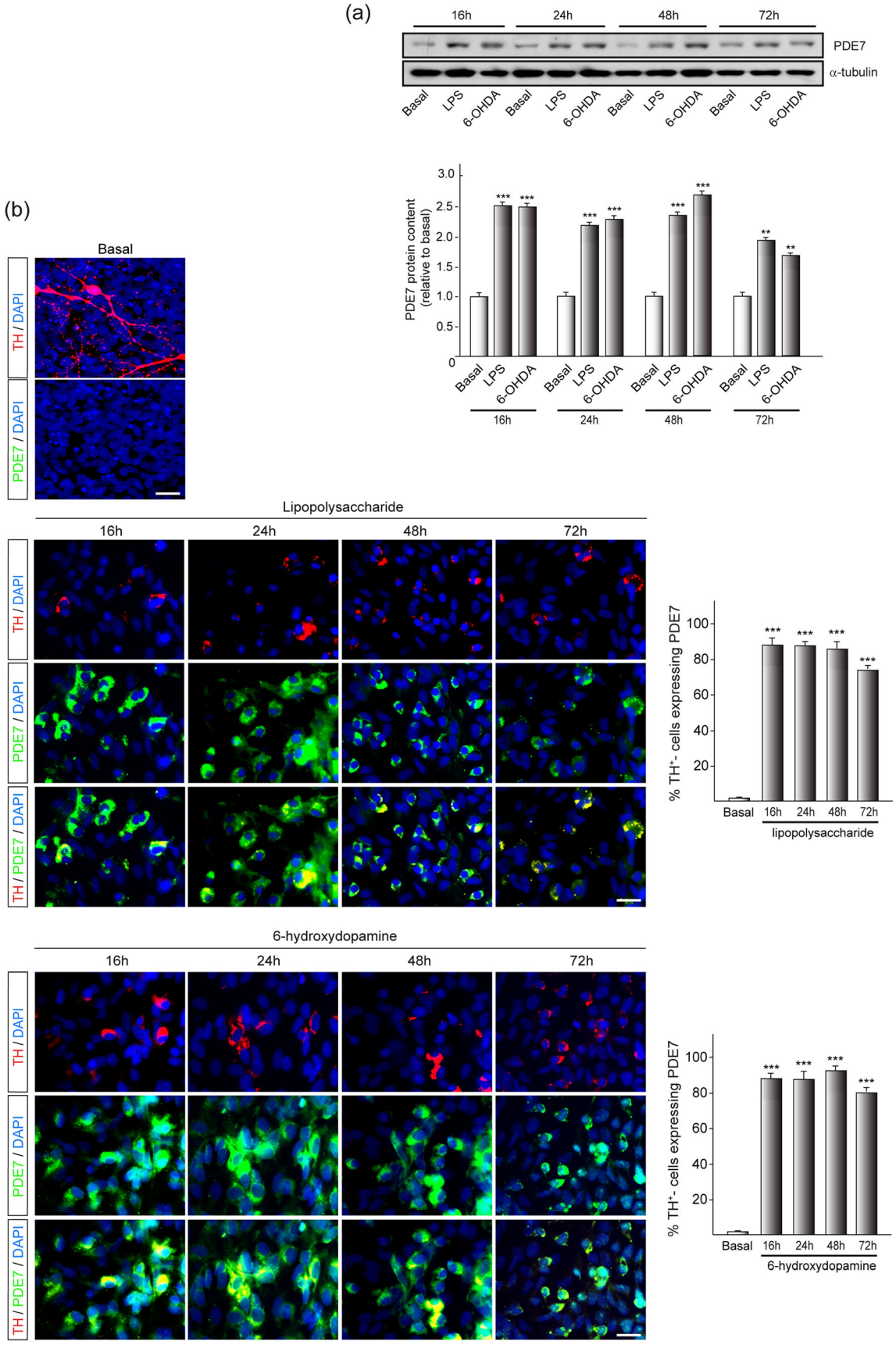
(a)
16h
24h
48h
72h
PDE7
α-tubulin
Basal
LPS
6-OHDA
PDE7 protein content (relative to basal)
(b)
Basal
TH / DAPI
PDE7 / DAPI
TH / PDE7 / DAPI
Lipopolysaccharide
% TH+- cells expressing PDE7
lipopolysaccharide
6-hydroxydopamine

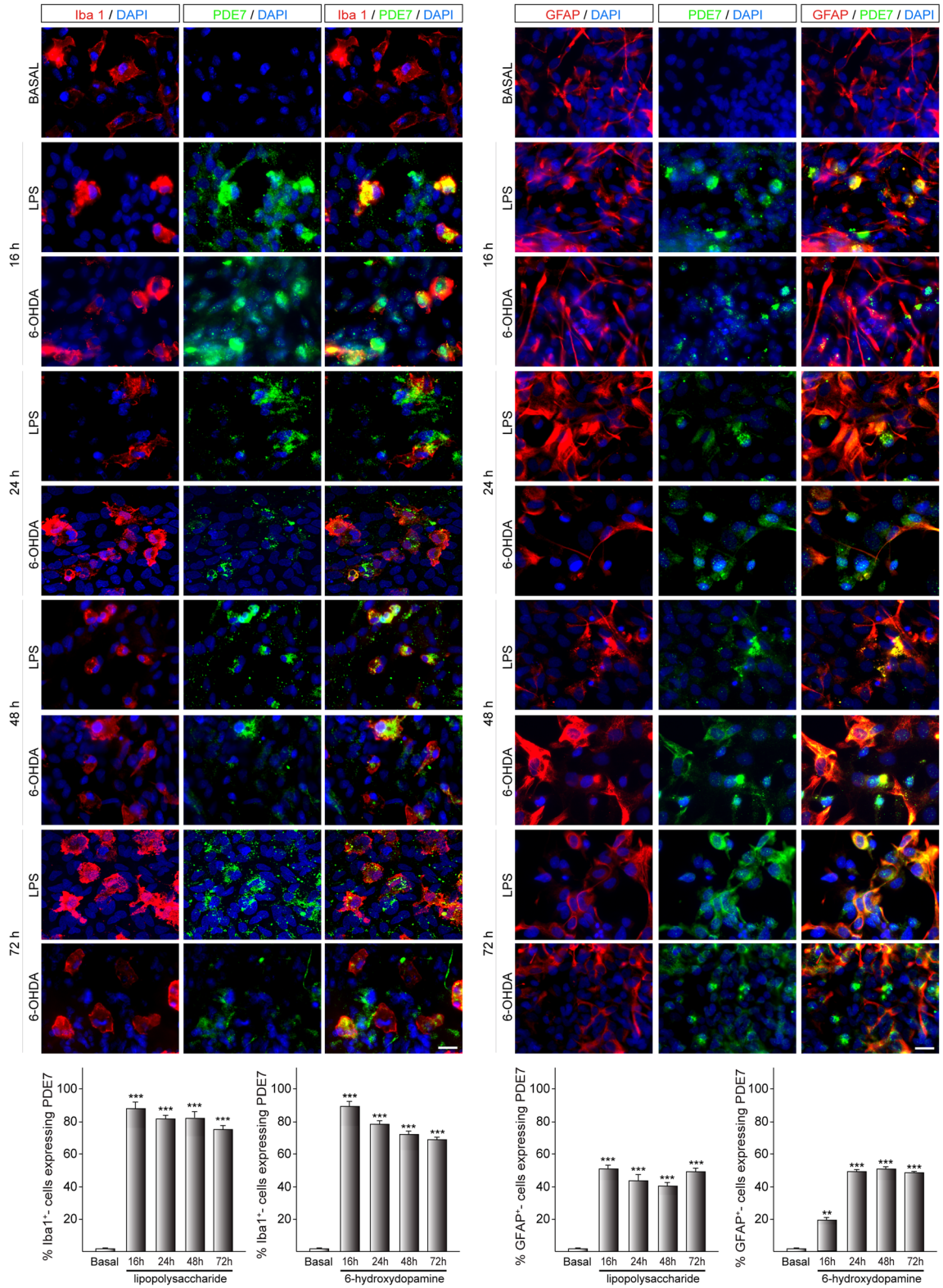

Fig. 3 PDE7 expression on glial cells in embryonic mesencephalic-derived cultures after damage. Primary mesencephalic-derived cultures were treated with LPS (10 μg/ml) or 6-OHDA (35 μM) and the expression of PDE7 (green) after damage at indicated times determined by immunofluorescence. PDE7 expression in microglial cells (Iba1-positive cells, red) and astroglial cells (GFAP-expressing cells, red) was evaluated and quantified. Nuclei were counterstained with DAPI (blue). Representative images of at least three independent experiments are shown. Scale bar, 20 μm. The bar graphs show the percentage of total microglial ($Iba1^+$) and/or astroglial ($GFAP^+$) cells co-expressing PDE7 after LPS or 6-OHDA exposure. $***p \leq 0.001$; $**p \leq 0.01$ (basal-compared)

immunocytochemistry and Western blot. In response to different stimuli, such as LPS or 6-OHDA, glial cells become activated and undergo morphological as well as functional alterations [36]. As expected, in our model, exposure of glial cells to damage induced morphological changes compatible with microglia and astroglia reactivity. Under stimulating conditions, microglial cells become irregular with an ameboid shape, while astrocytes present thickened surfaces and shortening of cytoplasmic projections (Fig. 4). These changes are characteristic of reactive cells. As shown in Fig. 4a, immunocytochemistry analysis revealed reactive microglial cells expressing PDE7 after LPS exposure at all stages treated. Interestingly, PDE7 level quantification, as measured by Western blot, increased notably in microglia after LPS exposure (Fig. 4b) starting from 16 h. Similar results were observed in astroglial cultures (Fig. 4c and d) with an increase of the expression of PDE7 after damage in astrocytes as observed by immunocytochemistry (Fig. 4c). Quantification of PDE7 levels in astroglial cells (Fig. 4d) confirmed this increase after insult although PDE7 expression seemed to be lower, in comparison with microglia, and also starts later.

PDE7 Expression Is Increased in the *Substantia nigra* pars compacta in Preclinical Models of PD

In view of the above-described results suggesting a role of PDE7 on neurodegeneration and neuroinflammation processes, we next examined PDE7 protein levels in two clinically relevant in vivo models of PD. Adult rats were injected into the *SNpc* with LPS (neuroinflammatory model) or 6-OHDA (oxidative stress model), and the expression of PDE7 was evaluated 72 h after intracranial injection. Brain examinations revealed, as expected, a loss of dopaminergic cells after injury, which was paralleled by an enhanced expression of the PDE7 protein (Fig. 5). Since PDE7-mediated cAMP level decrease may interfere with dopaminergic signaling, we next measured the expression of TH, DAT, and DARPP32 in the striatum. DAT is a dopamine transporter expressed in striatal axon terminals [37] and DARPP32 is a marker of dopaminoceptive neuros [38]. Figure 5b clearly shows that following the unilaterally delivery of LPS and 6-OHDA in the *SNpc*, the degeneration of TH^+ fibers in the striatum began immediately. This rapid loss of dopaminergic fibers is in accordance with the loss of striatal DAT-positive fibers. Interestingly, we can also find a decrease in the immunostaining of DARPP-32 fibers.

In order to analyze whether the increase in PDE7 expression took place in dying neurons, we performed immunofluorescence analysis using anti-active caspase-3, anti-TH, and anti-PDE7 specific antibodies on brain sections containing the *SNpc* of animals injected with LPS or 6-OHDA (Fig. 6). Representative images show that in the *SNpc*, those dopaminergic neurons closest to the ventral tegmental area did not show any cellular damage at the time analyzed. They expressed neither PDE7 nor caspase 3. On the contrary, those neurons closest to the *pars lateralis* seemed to be degenerating and presented a shrinking morphology (white arrows). In these neurons that exhibited greater dopaminergic damage, we observed an induction on the expression levels of active caspase-3 as well as PDE7, suggesting that, indeed, PDE7 expression is induced in those cells that are degenerating.

Next, we examined PDE7 expression in the activated glial cells present in the two PD animal models used (Fig. 7). In vehicle-injected animals, *SNpc* displays ramified Iba-1 positive cells with two or three fine processes, a morphology consistent with resting microglial cells. As expected 72 h after intracerebral LPS or 6-OHDA injection, the number of Iba1-positive cells was highly increased, and the majority of these microglial cells did not show ramified but a round morphology, characteristic of a microglial-activated state (Fig. 7a). When PDE7 expression was evaluated, higher levels were found 72 h after damage, both in the neuroinflammation (LPS-injection) and in the oxidative stress (6-OHDA injection) animal models. As shown in Fig. 7a, most of the PDE7 was located in the *SNpc*, in those microglial cell–enriched areas surrounding the dopaminergic neurons, and particularly in the hyperactivated microglial cells. The same results were observed in areas of the *SNpc* containing astrocytes. After damage, astrocytes modify their characteristic morphology, appearing as round thickened cells with shortened condensed processes (Fig. 7b) and a higher expression of GFAP was also observed. At this hyperactivation state, many of them also expressed high levels of PDE7.

PDE7 Promoter Activity in Transfected Dopaminergic Cell Line and Primary Glial Cells after Damage

To further analyze the regulation of PDE7 by 6-OHDA and LPS, we next performed transient transfection experiments on the dopaminergic cell line SH-SY5Y and on primary glial cultures isolated from adult rats. To that end, we analyzed the expression of a fragment of 962 bp of the *Homo sapiens* PDE7 promoter (plus 109 bp of the first exon). Figure 8a shows the results obtained when transfecting SH-SY5Y cells with a construction containing this fragment (PDE7/1071) with/without 6-OHDA treatment. As can be seen, there is a significant increase in the relative luciferase activity in those cells transfected with the PDE7/1071 construct, compared with the basal values, arbitrarily assigned with the value 1 (cells transfected with the empty Pxp1 vector), and these values were significantly increased in those cultures treated with 6-OHDA. Next, we analyzed the effect of LPS in primary cultures of microglial cells (Fig. 8b) and astrocytes (Fig. 8c), isolated from adult rats. As can be seen, and as it happened with 6-OHDA, treatment of glial cultures with LPS resulted in a significant increase of PDE7 promoter activity, as compared

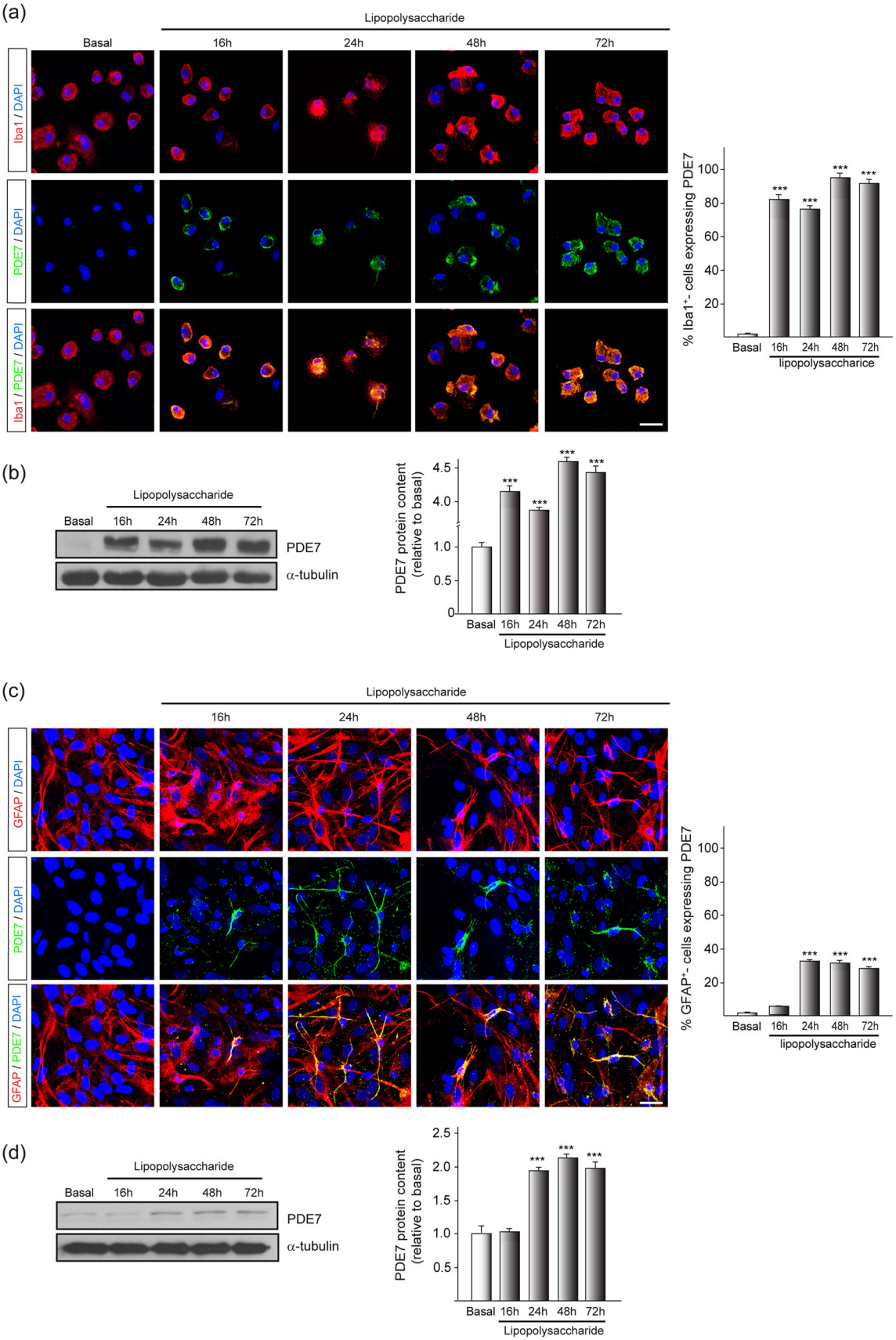
(a)
Lipopolysaccharide
Basal
16h
24h
48h
72h
Iba1 / DAPI
PDE7 / DAPI
Iba1 / PDE7 / DAPI
% Iba1+- cells expressing PDE7
Basal 16h 24h 48h 72h
lipopolysaccharice
(b)
Lipopolysaccharide
Basal 16h 24h 48h 72h
PDE7
α-tubulin
PDE7 protein content (relative to basal)
Basal 16h 24h 48h 72h
Lipopolysaccharide
(c)
Lipopolysaccharide
16h
24h
48h
72h
GFAP / DAPI
PDE7 / DAPI
GFAP / PDE7 / DAPI
% GFAP+- cells expressing PDE7
Basal 16h 24h 48h 72h
lipopolysaccharide
(d)
Lipopolysaccharide
Basal 16h 24h 48h 72h
PDE7
α-tubulin
PDE7 protein content (relative to basal)
Basal 16h 24h 48h 72h
Lipopolysaccharide

◀ **Fig. 4** PDE7 expression on primary glial cultures after damage. Primary glial cultures were treated with LPS (10 μg/ml) at indicated times. **a** PDE7 expression (green) analysis by immunofluorescence and quantification in microglial cells (Iba1-expressing cells, red). Nuclei were counterstained with DAPI (blue). Representative images of at least three independent experiments are shown. Scale bar, 20 μm. The bar graphs show the percentage of total microglial ($Iba1^+$) cells co-expressing PDE7 after damage. **b** Representative Western blot and quantification analysis showing expression levels of PDE7 in microglial cells after LPS exposure. **c** PDE7 expression (green) and quantification in astroglial cells (GFAP-positive cells, red). Nuclei were counterstained with DAPI (blue). Representative images of at least three independent experiments are shown. Scale bar, 20 μm. The bar graphs show the percentage of total astroglial ($GFAP^+$) cells co-expressing PDE7 after insult. **d** Representative Western blot and quantification analysis showing expression levels of PDE7 in astroglial cells after LPS exposure at indicated times. ***$p \leq 0.001$ (basal-compared)

with the values obtained with the empty vector. These results indicate that PDE7 expression is directly upregulated after an oxidative stress as well as after an inflammatory injury.

Discussion

PD is the most predominant movement disorder, characterized by the loss of dopaminergic neurons in the *pars compacta* of the *Substantia nigra* that leads to a reduced facilitation of voluntary movements. Although levodopa treatment mitigates some of the motor symptoms of PD, thanks to the dopamine replacement, therefore contributing to improve the quality of life of patients, so far there is no treatment that forestalls the progressive degeneration of dopaminergic neurons [39], indicating that new targets and novel therapeutic strategies to inhibit this disease ought to be considered. In line with this, up to now, the precise mechanisms responsible for progression of neurodegenerative diseases remain elusive, being chronic neuroinflammation as one of the most prominent features shared by several neurodegenerative diseases, included PD [6–8], playing an important role in the onset and progression of the diseases [9].

PDE enzymes selectively degrade cAMP and/or cGMP, one of the most important intracellular messengers, regulating the intracellular concentrations of these cyclic nucleotides, their signaling pathways, and therefore countless biological responses in health and disease. Consequently, therapeutic effects of PDEs inhibitors have been widely investigated, being the subject of numerous studies to prove their effectiveness in the treatment of several pathologies like heart failure (PDE3 inhibitor), severe chronic obstructive pulmonary disease (PDE4 inhibitors), pulmonary hypertension, or erectile dysfunction (PDE5 inhibitors) [40]. In recent years, some other different isoforms of PDEs are drawing the attention of the scientific community looking for novel therapeutic targets against neurodegenerative disorders [41–43]. In relationship with PD, the inhibition of PDE4, PDE7, and PDE10 seems to be involved in protecting dopaminergic neurons and/or sustaining dopaminergic tone in PD models [44]. Our group was the first to demonstrate a potent neuroprotective and anti-inflammatory effect of PDE7 inhibition in different models of neurodegenerative diseases, including Alzheimer's disease [45], spinal cord injury [46], stroke [47], autoinmune encephalomyelitis [48], multiple sclerosis [49], and PD using several approaches, such as chemical inhibition [24] as well as genetic depletion [50]. However, up to now, very little is known regarding the physiological role of PDE7 and its implication in the onset and progression of neurodegenerative diseases. Also, little is known about the subcellular distribution of PDE7 in specific cells types. In this work, we demonstrate for the first time that PDE7 expression is upregulated in in vitro and in vivo models of PD, which suggests that this enzyme plays an important role in the progress of the disease. Previous studies about PDE7 location in brain are based on in situ hybridization as well as RT-PCR studies [22, 23, 51, 52]. Some preliminary observations derived from studies of our group, based on the use of PDE7 inhibitors, suggested an increase in the expression of PDE7 in the *SNpc* of parkinsonian rats [50]. Moreover, previous to this work, we had observed in vitro the presence of PDE7 in the cytoplasm of the dopaminergic cell line SH-SY5Y and in primary mesencephalic cultures [24]. In this work, in vitro experiments, using the human dopaminergic cell line SH-SY5Y and embryonic mesencephalic primary cultures, reveal an early PDE7 activation shortly after damage, remaining high some hours later. Similarly, results derived from in vivo analysis show an increase in the expression of PDE7 in the *SNpc*, as a consequence of the damage induced by 6-OHDA and/or LPS. However, the increase in PDE7 expression is not homogeneous throughout the entire *SNpc*. Increased PDE7 expression after damage is mainly located in those areas of the *SNpc* containing a large amount of degenerating dopaminergic neurons that also express apoptotic markers such as activated caspase-3.

The early activation of PDE7 here described may result in the onset and/or progression of PD leading to the degeneration of dopaminergic neurons. We have observed similar results in vitro in the dopaminergic cell line SH-SY5Y after 6-OHDA exposure, with degenerating neurons also expressing active caspase-3 and annexin V [24], and agrees with previous observations by our group [24, 50] demonstrating that activation of this enzyme occurs within a few hours after neuronal damage and is maintained over the 72 h period following insult. This fact could be really important in the early diagnosis of PD, since the activation of PDE7 could be a primary trigger of neuronal damage.

It has been shown that PDE7 is involved in pro-inflammatory processes and could be a target for the control

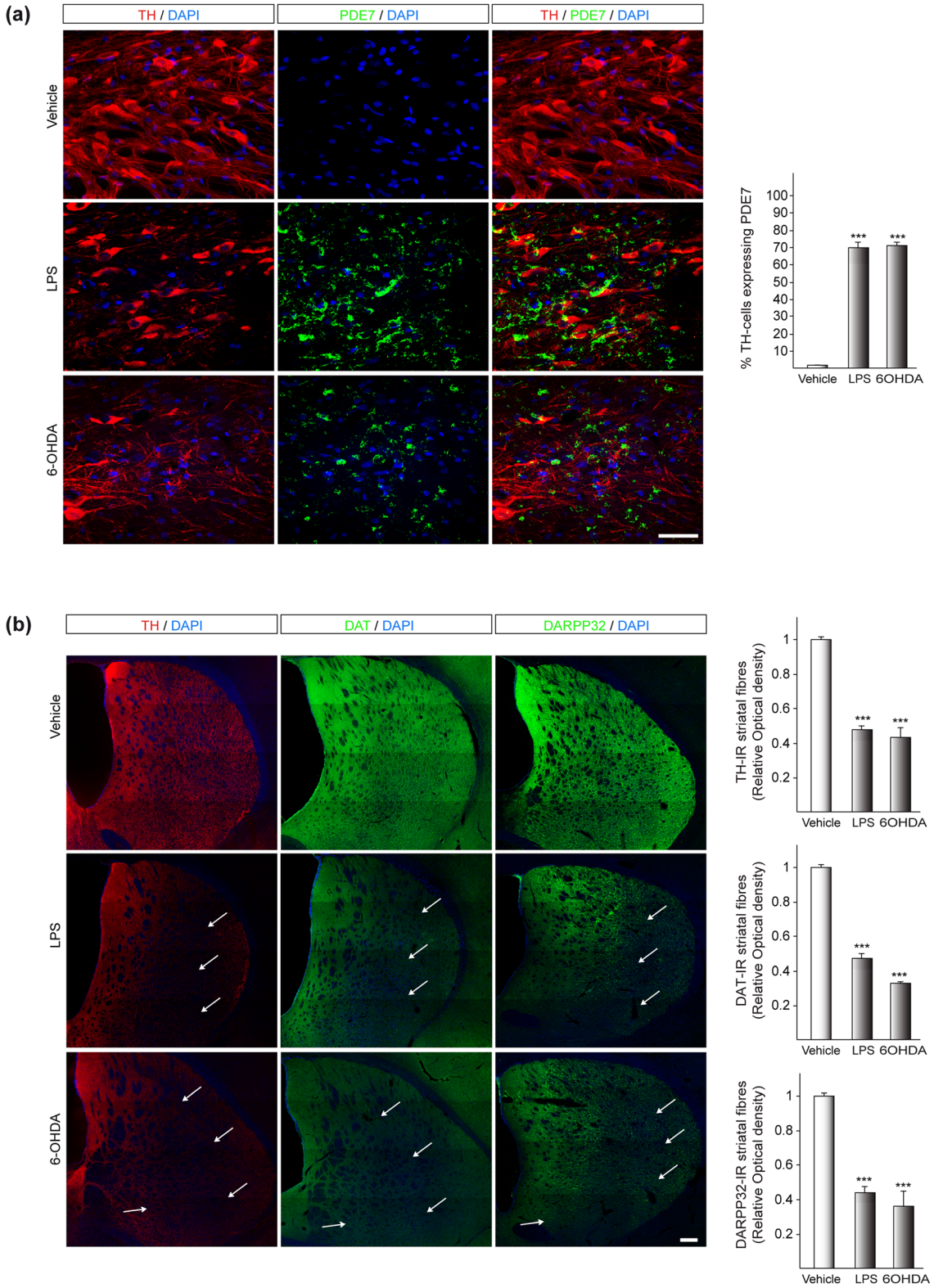

Fig. 5 In vivo PDE7 expression in dopaminergic neurons of the *Substantia nigra pars compacta* after intracerebral damage. Dopaminergic striatal alterations. LPS (10 μg) or 6-OHDA (9 μg) was injected unilaterally into the *Substantia nigra pars compacta* (SNpc) of adult rats and after 72 h, the brains were removed and tissue sections were processed. **a** Immunofluorescence analysis showing the expression of PDE7 (green) in dopaminergic neurons (tyrosine hydroxylase, TH, red) in the SNpc after damage. Scale bars, 50 μm. Quantification of dopaminergic cells (TH-immunoreactive) expressing PDE7 is shown. ***$p \leq 0.001$ (vehicle-compared). **b** Representative stitched images (tile scan) of TH-, DAT-, and DARPP32-immunoreactive (IR) fibers in the striatum. Arrows represent areas of loss of IR fibers. Optical density analysis for every given marker is shown. ***$p < 0.001$ (vehicle-compared). Scale bar, 250 μm

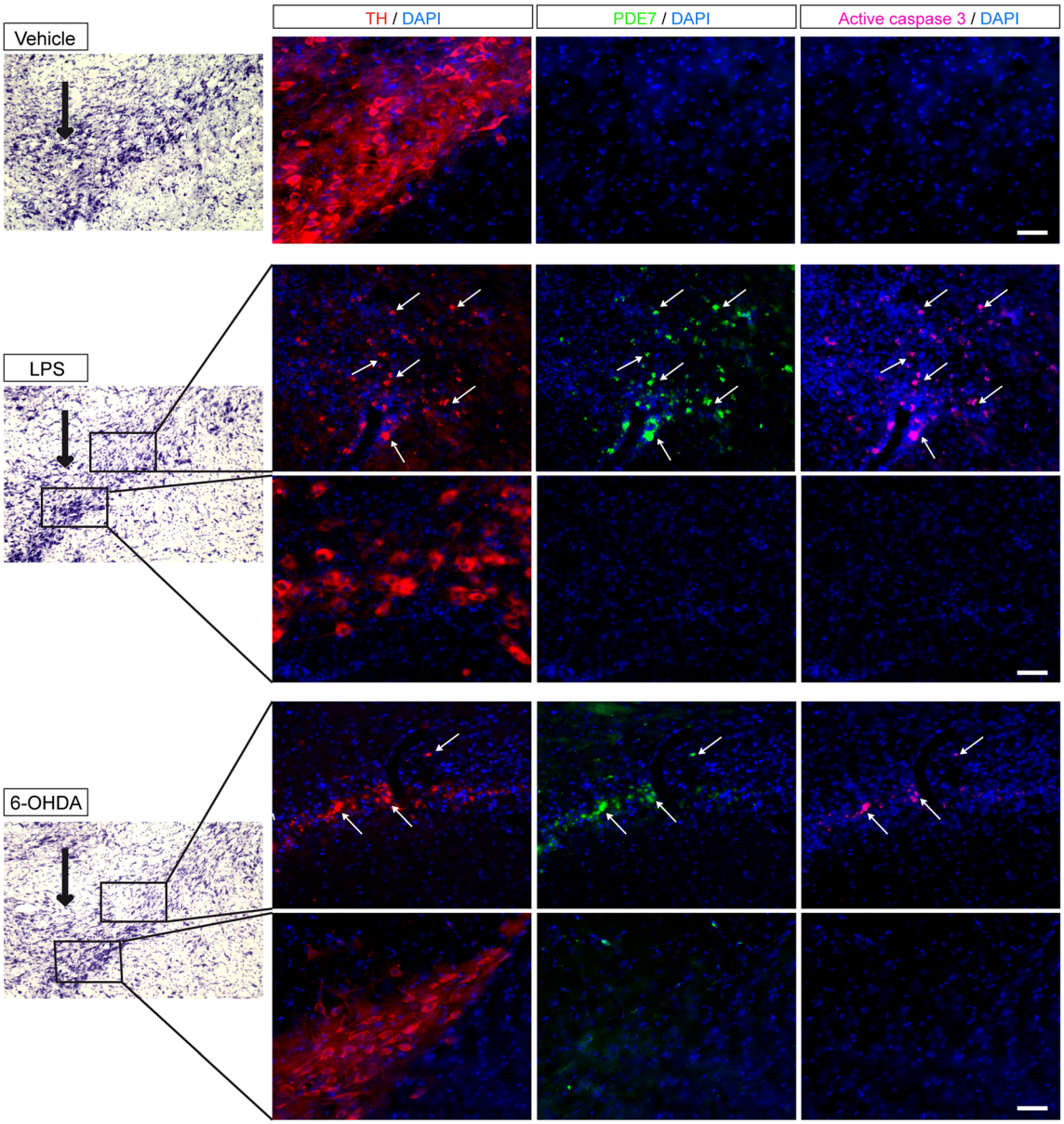

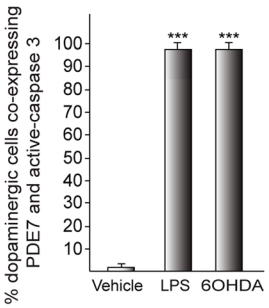

Fig. 6 In vivo PDE7 and active caspase-3 co-expression in dopaminergic neurons of the *Substantia nigra pars compacta* after intracerebral damage. LPS (10 μg) or 6-OHDA (9 μg) was injected unilaterally into the adult *Substantia nigra pars compacta* (SNpc) of adult rats and after 72 h, the brains were removed and tissue sections were processed. Nissl stained images show those areas of the SNpc used for immunofluorescence analysis. Confocal representative images showing the co-expression (arrows) of PDE7 (green) and active caspase-3 (magenta) in dopaminergic neurons (tyrosine hydroxylase immunoreactive cells, TH, red) in the SNpc after damage. Scale bars, 50 μm. Quantification of apoptotic (active caspase 3 expressing cells) dopaminergic cells (TH-immunoreactive) is shown. ***$p \leq 0.001$ (vehicle-compared)

of this process [45, 53]. Additionally, PDE7 is necessary for the induction of T cell proliferation [54]. All these data, together with the results here described support our initial hypothesis that PDE7 is responsible to some extent for the progressive neuronal damage that occurs in neurodegenerative disorders, in part due to the regulation of neuroinflammation, suggesting that that PDE7 can be an important agent in the progression of PD. In point of fact, we observed a clear induction of PDE7 expression, mainly in microglial cells, both in vitro and in vivo, suggesting that the expression of this enzyme is important for

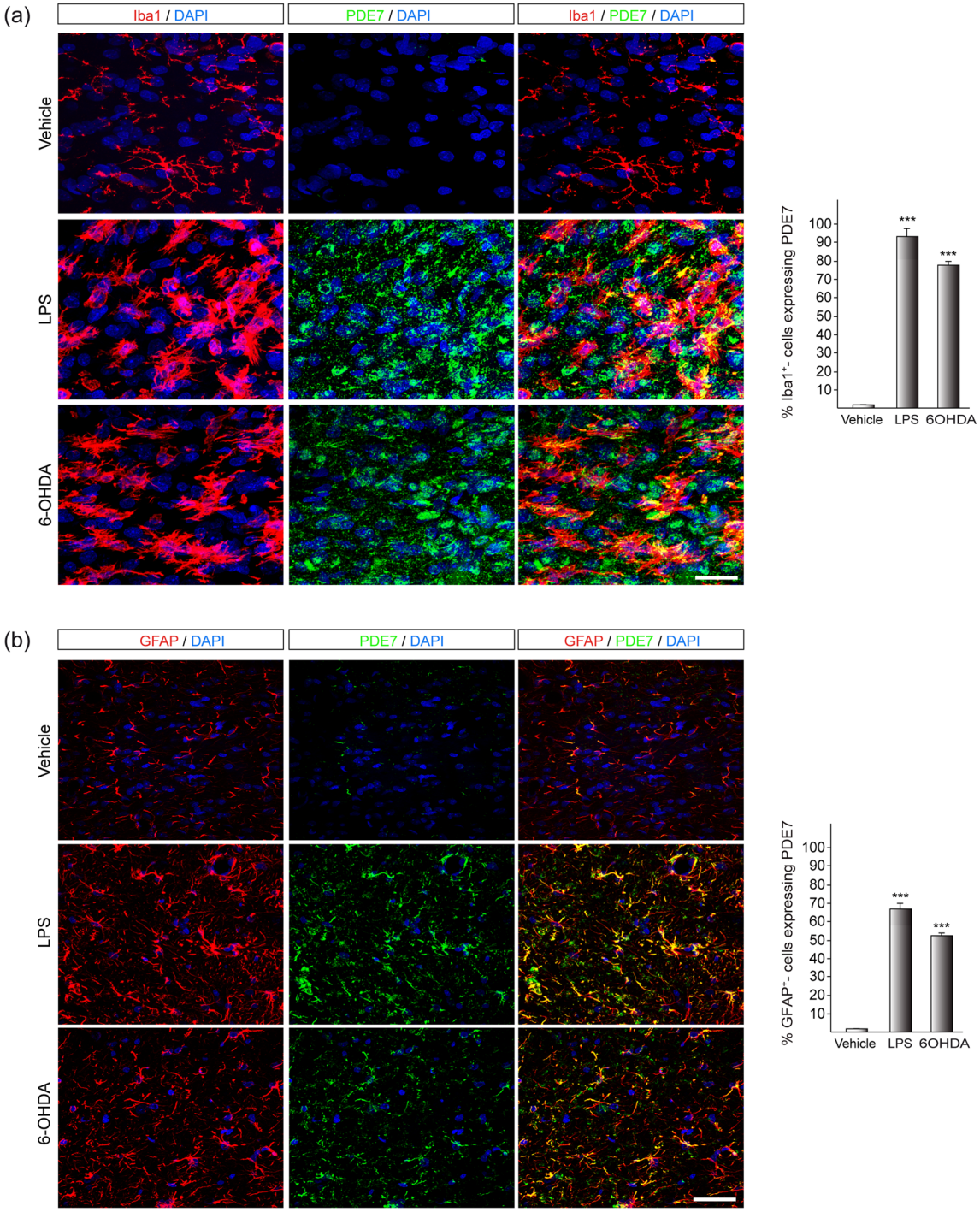

Fig. 7 PDE7 expression in glial cells in the *Substantia nigra pars compacta* after intracerebral damage. LPS (10 μg) or 6-OHDA (9 μg) was injected unilaterally into the adult *Substantia nigra pars compacta* (SNpc) of adult rats and after 72 h, the brains were removed and tissue sections were processed. Immunofluorescence analysis showing the expression of PDE7 (green) in microglial cells (Iba-1-expressing cells, red) (**a**) and astroglial cells (GFAP-positive cells, red) (**b**) in the SNpc after damage. Scale bars, 50 μm. Quantification of microglial cells (Iba1-immunoreactive) and astrocytes (GFAP-positive cells) expressing PDE7 is shown. ***$p \leq 0.001$ (vehicle-compared)

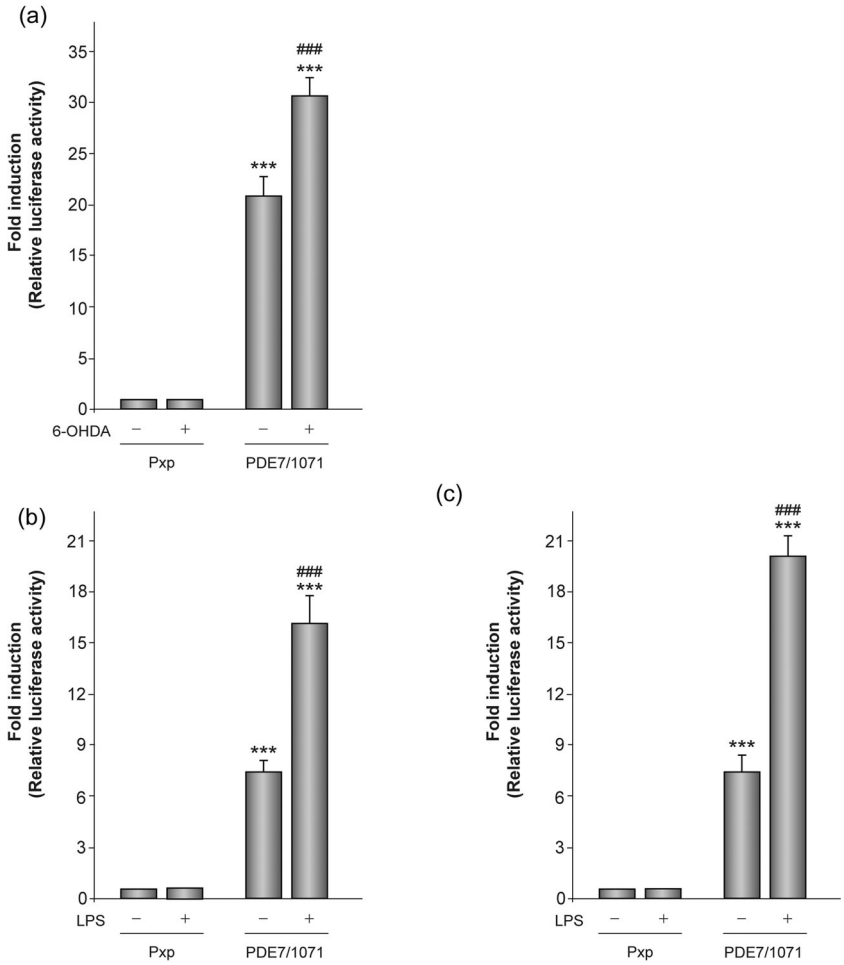

Fig. 8 Study in vitro of the PDE7 promotor activity. Transient transfection experiments. The entire promoter fragment (PDE7/1071) was subcloned in the promoterless luciferase reporter vector pxp1 (Pxp) and transfected into the dopaminergic cell line SH-SY5Y (**a**), in rat primary microglial cells (**b**), and in astrocyte cultures (**c**). SH-SY5Y cells were then treated with 6-OHDA (35 μM) and glial cells with LPS (10 μg/ml) during 24 h. Data are expressed relative to basal values and represented as the mean ± SD of luciferase activity determined in triplicate in at least three independent experiments. $^{***}p < 0.001$ versus basal cultures; $^{###}p < 0.001$ versus PDE7/1071 promotor-transfected cells

the neuroinflammatory response triggered by these cells leading to an increase in the degeneration of dopaminergic neurons.

Regarding PDE7 transcriptional regulation by 6-OHDA and LPS, transient transfection experiments with a fragment of the *PDE7* promoter region (PDE7/1071) revealed that neurons and glial cells exposed to these agents result in a significant induction in the expression of PDE7 promoter, suggesting that PDE7 activity is directly upregulated by both compounds. Certainly, more experiments are needed in order to define the regulatory regions in the *PDE7* gene promoter responsible for this regulation.

Collectively, our findings clearly support the suggestion that the expression of PDE7 increases in dopaminergic neurons and glial cells after inducing an oxidative stress process or following a pro-inflammatory stimulus in in vitro and in vivo models of PD. Therefore, PDE7 could play an important role in the onset and/or progression of the disease. These data provide constraining reasons to identify new drugs, which selectively target PDE7, preventing the PD progression.

Acknowledgments We thank Monica Belinchon, expert in confocal images, for her technical support with the confocal microscope and Victor Echeverry, Jose Antonio Lopez-Moreno and Manuel Guzman from the Complutense University for kindly providing us with DAT and DARPP32 antibodies.

Funding Information This work was financially supported by the Spanish Ministry of Economy and Competitiveness (grants SAF2014-52940-R and SAF2017-85199-P to A.P-C) and partially financed with FEDER funds. The Network Center for Biomedical Research in Neurodegenerative Diseases (CIBERNED) is funded by the Institute for Health "Carlos III." J.A.M-G. is a post-doctoral fellow from CIBERNED.

Compliance with Ethical Standards

All applicable international, national, and/or institutional guidelines for the care and use of animals were followed. All animal experiments were specifically approved by the "Ethics Committee for Animal Experimentation" of the Instituto de Investigaciones Biomedicas (CSIC-UAM) and carried out in accordance with the European Communities Council Directive (2010/63/EEC) and National regulations (normative 53/2013).

Conflict of Interest The authors declare that they have no conflict of interest.

References

1. Michel PP, Hirsch EC, Hunot S (2016) Understanding dopaminergic cell death pathways in Parkinson disease. Neuron 90(4):675–691. https://doi.org/10.1016/j.neuron.2016.03.038

2. Kulkarni OP, Lichtnekert J, Anders HJ, Mulay SR (2016) The immune system in tissue environments regaining homeostasis after injury: is "inflammation" always inflammation? Mediat Inflamm 2016:2856213. https://doi.org/10.1155/2016/2856213
3. Shabab T, Khanabdali R, Moghadamtousi SZ, Kadir HA, Mohan G (2017) Neuroinflammation pathways: a general review. Int. J. Neurosci. 127(7):624–633. https://doi.org/10.1080/00207454.2016.1212854
4. Ransohoff RM (2016) How neuroinflammation contributes to neurodegeneration. Science 353(6301):777–783. https://doi.org/10.1126/science.aag2590
5. Russo MV, McGavern DB (2016) Inflammatory neuroprotection following traumatic brain injury. Science 353(6301):783–785. https://doi.org/10.1126/science.aaf6260
6. Colonna M, Butovsky O (2017) Microglia function in the central nervous system during health and neurodegeneration. Annu Rev Immunol 35:441–468. https://doi.org/10.1146/annurev-immunol-051116-052358
7. Perry VH, Nicoll JA, Holmes C (2010) Microglia in neurodegenerative disease. Nat Rev Neurol 6(4):193–201. https://doi.org/10.1038/nrneurol.2010.17
8. Hirsch EC, Vyas S, Hunot S (2012) Neuroinflammation in Parkinson's disease. Parkinsonism Relat Disord 18(Suppl 1): S210–S212. https://doi.org/10.1016/S1353-8020(11)70065-7
9. Chen WW, Zhang X, Huang WJ (2016) Role of neuroinflammation in neurodegenerative diseases (review). Mol Med Rep 13(4):3391–3396. https://doi.org/10.3892/mmr.2016.4948
10. Heneka MT, Kummer MP, Latz E (2014) Innate immune activation in neurodegenerative disease. Nat Rev Immunol 14(7):463–477. https://doi.org/10.1038/nri3705
11. Pal R, Tiwari PC, Nath R, Pant KK (2016) Role of neuroinflammation and latent transcription factors in pathogenesis of Parkinson's disease. Neurol Res 38(12):1111–1122. https://doi.org/10.1080/01616412.2016.1249997
12. Tansey MG, McCoy MK, Frank-Cannon TC (2007) Neuroinflammatory mechanisms in Parkinson's disease: potential environmental triggers, pathways, and targets for early therapeutic intervention. Exp Neurol 208(1):1–25. https://doi.org/10.1016/j.expneurol.2007.07.004
13. Conti M, Beavo J (2007) Biochemistry and physiology of cyclic nucleotide phosphodiesterases: essential components in cyclic nucleotide signaling. Annu Rev Biochem 76:481–511. https://doi.org/10.1146/annurev.biochem.76.060305.150444
14. Bender AT, Beavo JA (2006) Cyclic nucleotide phosphodiesterases: molecular regulation to clinical use. Pharmacol Rev 58(3):488–520. https://doi.org/10.1124/pr.58.3.5
15. Kelly MP (2018) Cyclic nucleotide signaling changes associated with normal aging and age-related diseases of the brain. Cell Signal 42:281–291. https://doi.org/10.1016/j.cellsig.2017.11.004
16. Ffytche DH, Creese B, Politis M, Chaudhuri KR, Weintraub D, Ballard C, Aarsland D (2017) The psychosis spectrum in Parkinson disease. Nat Rev Neurol 13(2):81–95. https://doi.org/10.1038/nrneurol.2016.200
17. Lugnier C (2006) Cyclic nucleotide phosphodiesterase (PDE) superfamily: a new target for the development of specific therapeutic agents. Pharmacol Ther 109(3):366–398. https://doi.org/10.1016/j.pharmthera.2005.07.003
18. Dyke HJ, Montana JG (2002) Update on the therapeutic potential of PDE4 inhibitors. Expert Opin Investig Drugs 11(1):1–13. https://doi.org/10.1517/13543784.11.1.1
19. Spina D (2003) Phosphodiesterase-4 inhibitors in the treatment of inflammatory lung disease. Drugs 63(23):2575–2594. https://doi.org/10.2165/00003495-200363230-00002
20. Bloom TJ, Beavo JA (1996) Identification and tissue-specific expression of PDE7 phosphodiesterase splice variants. Proc Natl Acad Sci U S A 93(24):14188–14192
21. Sasaki T, Kotera J, Omori K (2002) Novel alternative splice variants of rat phosphodiesterase 7B showing unique tissue-specific expression and phosphorylation. Biochem. J. 361 (Pt 2:211–220
22. Miro X, Perez-Torres S, Palacios JM, Puigdomenech P, Mengod G (2001) Differential distribution of cAMP-specific phosphodiesterase 7A mRNA in rat brain and peripheral organs. Synapse 40(3): 201–214. https://doi.org/10.1002/syn.1043
23. Reyes-Irisarri E, Perez-Torres S, Mengod G (2005) Neuronal expression of cAMP-specific phosphodiesterase 7B mRNA in the rat brain. Neuroscience 132(4):1173–1185. https://doi.org/10.1016/j.neuroscience.2005.01.050
24. Morales-Garcia JA, Redondo M, Alonso-Gil S, Gil C, Perez C, Martinez A, Santos A, Perez-Castillo A (2011) Phosphodiesterase 7 inhibition preserves dopaminergic neurons in cellular and rodent models of Parkinson disease. PLoS One 6(2):e17240. https://doi.org/10.1371/journal.pone.0017240
25. Morales-Garcia JA, Alonso-Gil S, Gil C, Martinez A, Santos A, Perez-Castillo A (2015) Phosphodiesterase 7 inhibition induces dopaminergic neurogenesis in hemiparkinsonian rats. Stem Cells Transl Med 4(6):564–575. https://doi.org/10.5966/sctm.2014-0277
26. Morales-Garcia JA, Echeverry-Alzate V, Alonso-Gil S, Sanz-SanCristobal M, Lopez-Moreno JA, Gil C, Martinez A, Santos A et al (2017) Phosphodiesterase7 inhibition activates adult neurogenesis in hippocampus and subventricular zone in vitro and in vivo. Stem Cells 35(2):458–472. https://doi.org/10.1002/stem.2480
27. Bibb JA (2005) Decoding dopamine signaling. Cell 122(2):153–155. https://doi.org/10.1016/j.cell.2005.07.011
28. Sasaki T, Kotera J, Omori K (2004) Transcriptional activation of phosphodiesterase 7B1 by dopamine D1 receptor stimulation through the cyclic AMP/cyclic AMP-dependent protein kinase/cyclic AMP-response element binding protein pathway in primary striatal neurons. J Neurochem 89(2):474–483. https://doi.org/10.1111/j.1471-4159.2004.02354.x
29. Morales-Garcia JA, Palomo V, Redondo M, Alonso-Gil S, Gil C, Martinez A, Perez-Castillo A (2014) Crosstalk between phosphodiesterase 7 and glycogen synthase kinase-3: two relevant therapeutic targets for neurological disorders. ACS Chem Neurosci 5(3): 194–204. https://doi.org/10.1021/cn400166d
30. Morales-Garcia JA, de la Fuente RM, Alonso-Gil S, Rodriguez-Franco MI, Feilding A, Perez-Castillo A, Riba J (2017) The alkaloids of Banisteriopsis caapi, the plant source of the Amazonian hallucinogen Ayahuasca, stimulate adult neurogenesis in vitro. Sci Rep 7(1):5309. https://doi.org/10.1038/s41598-017-05407-9
31. Morales-Garcia JA, Gine E, Hernandez-Encinas E, Aguilar-Morante D, Sierra-Magro A, Sanz-SanCristobal M, Alonso-Gil S, Sanchez-Lanzas R et al (2017) CCAAT/Enhancer binding protein beta silencing mitigates glial activation and neurodegeneration in a rat model of Parkinson's disease. Sci Rep 7(1):13526. https://doi.org/10.1038/s41598-017-13269-4
32. Paxinos G, Watson C (2007) The rat brain in stereotaxic coordinates. 6th edn. Academic Press/Elsevier, Amsterdam
33. Barnes MJ, Cooper N, Davenport RJ, Dyke HJ, Galleway FP, Galvin FC, Gowers L, Haughan AF et al (2001) Synthesis and structure-activity relationships of guanine analogues as phosphodiesterase 7 (PDE7) inhibitors. Bioorg Med Chem Lett 11(8):1081–1083
34. Pitts WJ, Vaccaro W, Huynh T, Leftheris K, Roberge JY, Barbosa J, Guo J, Brown B et al (2004) Identification of purine inhibitors of phosphodiesterase 7 (PDE7). Bioorg Med Chem Lett 14(11):2955–2958. https://doi.org/10.1016/j.bmcl.2004.03.021
35. Vergne F, Bernardelli P, Lorthiois E, Pham N, Proust E, Oliveira C, Mafroud AK, Royer F et al (2004) Discovery of thiadiazoles as a novel structural class of potent and selective PDE7 inhibitors. Part 1: design, synthesis and structure-activity relationship studies.

Bioorg Med Chem Lett 14(18):4607–4613. https://doi.org/10.1016/j.bmcl.2004.07.008
36. Persson M, Brantefjord M, Hansson E, Ronnback L (2005) Lipopolysaccharide increases microglial GLT-1 expression and glutamate uptake capacity in vitro by a mechanism dependent on TNF-alpha. Glia 51(2):111–120. https://doi.org/10.1002/glia.20191
37. Hersch SM, Yi H, Heilman CJ, Edwards RH, Levey AI (1997) Subcellular localization and molecular topology of the dopamine transporter in the striatum and substantia nigra. J Comp Neurol 388(2):211–227
38. Anderson KD, Reiner A (1991) Immunohistochemical localization of DARPP-32 in striatal projection neurons and striatal interneurons: implications for the localization of D1-like dopamine receptors on different types of striatal neurons. Brain Res 568(1–2):235–243. https://doi.org/10.1016/0006-8993(91)91403-n
39. Obeso JA, Rodriguez-Oroz MC, Goetz CG, Marin C, Kordower JH, Rodriguez M, Hirsch EC, Farrer M et al (2010) Missing pieces in the Parkinson's disease puzzle. Nat Med 16(6):653–661. https://doi.org/10.1038/nm.2165
40. Maurice DH, Ke H, Ahmad F, Wang Y, Chung J, Manganiello VC (2014) Advances in targeting cyclic nucleotide phosphodiesterases. Nat Rev Drug Discov 13(4):290–314. https://doi.org/10.1038/nrd4228
41. Ribaudo G, Pagano MA, Bova S, Zagotto G (2016) New therapeutic applications of phosphodiesterase 5 inhibitors (PDE5-Is). Curr Med Chem 23(12):1239–1249
42. Li P, Zheng H, Zhao J, Zhang L, Yao W, Zhu H, Beard JD, Ida K et al (2016) Discovery of potent and selective inhibitors of phosphodiesterase 1 for the treatment of cognitive impairment associated with neurodegenerative and neuropsychiatric diseases. J Med Chem 59(3):1149–1164. https://doi.org/10.1021/acs.jmedchem.5b01751
43. Soares LM, Meyer E, Milani H, Steinbusch HW, Prickaerts J, de Oliveira RM (2017) The phosphodiesterase type 2 inhibitor BAY 60-7550 reverses functional impairments induced by brain ischemia by decreasing hippocampal neurodegeneration and enhancing hippocampal neuronal plasticity. Eur J Neurosci 45(4):510–520. https://doi.org/10.1111/ejn.13461
44. Nthenge-Ngumbau DN, Mohanakumar KP (2018) Can cyclic nucleotide phosphodiesterase inhibitors be drugs for Parkinson's disease? Mol Neurobiol 55(1):822–834. https://doi.org/10.1007/s12035-016-0355-8
45. Perez-Gonzalez R, Pascual C, Antequera D, Bolos M, Redondo M, Perez DI, Perez-Grijalba V, Krzyzanowska A et al (2013) Phosphodiesterase 7 inhibitor reduced cognitive impairment and pathological hallmarks in a mouse model of Alzheimer's disease. Neurobiol Aging 34(9):2133–2145. https://doi.org/10.1016/j.neurobiolaging.2013.03.011
46. Paterniti I, Mazzon E, Gil C, Impellizzeri D, Palomo V, Redondo M, Perez DI, Esposito E et al (2011) PDE 7 inhibitors: new potential drugs for the therapy of spinal cord injury. PLoS One 6(1):e15937. https://doi.org/10.1371/journal.pone.0015937
47. Redondo M, Zarruk JG, Ceballos P, Perez DI, Perez C, Perez-Castillo A, Moro MA, Brea J et al (2012) Neuroprotective efficacy of quinazoline type phosphodiesterase 7 inhibitors in cellular cultures and experimental stroke model. Eur J Med Chem 47(1):175–185. https://doi.org/10.1016/j.ejmech.2011.10.040
48. Martin-Alvarez R, Paul-Fernandez N, Palomo V, Gil C, Martinez A, Mengod G (2017) A preliminary investigation of phoshodiesterase 7 inhibitor VP3.15 as therapeutic agent for the treatment of experimental autoimmune encephalomyelitis mice. J Chem Neuroanat 80:27–36. https://doi.org/10.1016/j.jchemneu.2016.12.001
49. Mestre L, Redondo M, Carrillo-Salinas FJ, Morales-Garcia JA, Alonso-Gil S, Perez-Castillo A, Gil C, Martinez A et al (2015) PDE7 inhibitor TC3.6 ameliorates symptomatology in a model of primary progressive multiple sclerosis. Br J Pharmacol 172(17):4277–4290. https://doi.org/10.1111/bph.13192
50. Morales-Garcia JA, Aguilar-Morante D, Hernandez-Encinas E, Alonso-Gil S, Gil C, Martinez A, Santos A, Perez-Castillo A (2015) Silencing phosphodiesterase 7B gene by lentiviral-shRNA interference attenuates neurodegeneration and motor deficits in hemiparkinsonian mice. Neurobiol Aging 36(2):1160–1173. https://doi.org/10.1016/j.neurobiolaging.2014.10.008
51. Johansson EM, Reyes-Irisarri E, Mengod G (2012) Comparison of cAMP-specific phosphodiesterase mRNAs distribution in mouse and rat brain. Neurosci Lett 525(1):1–6. https://doi.org/10.1016/j.neulet.2012.07.050
52. Hoffmann R, Abdel'Al S, Engels P (1998) Differential distribution of rat PDE-7 mRNA in embryonic and adult rat brain. Cell Biochem Biophys 28(2–3):103–113. https://doi.org/10.1007/BF02737807
53. Giembycz MA, Smith SJ (2006) Phosphodiesterase 7A: a new therapeutic target for alleviating chronic inflammation? Curr Pharm Des 12(25):3207–3220
54. Nakata A, Ogawa K, Sasaki T, Koyama N, Wada K, Kotera J, Kikkawa H, Omori K et al (2002) Potential role of phosphodiesterase 7 in human T cell function: comparative effects of two phosphodiesterase inhibitors. Clin Exp Immunol 128(3):460–466